

## MICROSTRUCTURAL INVESTIGATION AND THERMAL STABILITY OF NANOCRYSTALLINE COCRFENI HIGH ENTROPY ALLOY

<sup>1</sup> Hasan KOTAN, <sup>2</sup> Recep C. KOÇ

<sup>1</sup> Bursa Technical University, Department of Metallurgical and Materials Engineering, Bursa, Türkiye, [hasan.kotan@btu.edu.tr](mailto:hasan.kotan@btu.edu.tr)

<sup>2</sup> Bursa Technical University, Graduate School, Department of Metallurgical & Materials Engineering, Bursa, Türkiye, [recepkanoc@gmail.com](mailto:recepkanoc@gmail.com)

<https://doi.org/10.37904/metal.2025.5075>

### Abstract

Although high entropy alloys (HEAs) have captured significant attention over the years, the nanocrystalline microstructure of HEAs, similar to that of conventional alloys, is unstable against grain growth. Our initial experimental results have revealed that the hardness of nanocrystalline CoCrFeNi HEA, measured as  $517.8 \pm 25$  HV, decreased substantially to  $221.5 \pm 11$  HV after 1 h of annealing at 1100 °C, and continued to decrease with prolonged annealing, reaching  $184 \pm 6.4$  HV as the annealing time was extended. This study has examined the effect of 1% and 2% Sm solute additions for structural stability and hardness changes of nanocrystalline CoCrFeNi HEAs upon temperature exposures up to 1100 °C and for durations up to 24 h. The structural analysis was performed using XRD as a function of annealing time and temperature, and mechanical changes were studied through hardness measurements. It was determined that Sm addition helps the CoCrFeNi HEA retain its high hardness even after 24 h of annealing at 900 °C. This is attributed to the presence of the rare earth element Sm and the formation of Sm-based mixed oxide phases.

**Keywords:** high entropy alloys, grain growth, annealing, hardness, thermal stability, nanocrystalline

### 1. INTRODUCTION

Nanocrystalline HEAs opens up new avenues for expanding their potential structural applications [1, 2]. Although synthesizing nanocrystalline HEAs using various techniques is relatively straightforward, preserving this fine-grained structure remains a considerable challenge [3]. That is, grain boundaries exhibit higher atomic disorders than grain interiors, and refined grain sizes in HEAs increase the total grain boundary area and lead to an increased free energy in their microstructures [4, 5]. Consequently, the decrease in this excess free energy creates a strong driving force for grain growth [6]. For example, while nanostructuring CoCrFeNi resulted in a threefold increase in hardness, subsequent annealing at 1100 °C for 24 h caused grain growth to 4.5 µm, leading to a 65% reduction in hardness [7-9]. It has been reported that introducing large solute atoms as solid solutions into nanocrystalline microstructures promotes their preferential segregation to grain boundaries [10], which consequently lowers the excess free energy or induces a solute drag effect, improving thermal stability [11]. Additionally, when added solute atoms form stable oxide phases upon high-temperature exposures, grain growth can be further reduced by impeding the grain boundaries through Zener pinning. For example, when alloyed with Y, CoCrFeNi HEA was reported to retain its nanocrystalline grain size after annealing at 900 °C [12]. The impact of Gd addition to CoCrCuFeNi HEA was investigated and reported an increase in hardness from 176 HV to 293 HV [13]. Moazzen et al. [14] studied thermal stability and mechanical properties of CoCrFeNi HEA with addition of 0.4% Zr, showing that the nanocrystalline structure could be retained at temperatures as high as 800 °C. Peng et al. [15] enhanced the microstructural stability and increased the mechanical properties of nanocrystalline CoCrFeNiMn HEA by adding Zr, Ti, and Y<sub>2</sub>O<sub>3</sub>.

In our previous study, we examined the effect of adding 4% Sm to CoCrFeNi HEA and achieved significant thermal stability after exposure to elevated temperatures [9]. In the present study, we aimed to investigate the effect of 1% and 2% Sm additions on the structural stability and hardness of nanocrystalline CoCrFeNi HEA as a function of annealing temperatures up to 1100 °C and annealing times up to 24 h.

## 2. MATERIALS AND METHODS

High-purity elemental powders were used to mechanically alloy (CoCrFeNi)<sub>100-x</sub>Sm<sub>x</sub> (x = 0, 1, and 2) HEAs using SPEX 8000 M/D high energy ball miller. The details of the mechanical alloying (MA) process are given elsewhere [9]. After the MA process, the samples were annealed at 700 °C, 900 °C and 1100 °C in an Ar protective atmosphere for 1, 3, 6, 12, and 24 h. The annealed HEAs were ground and polished for subsequent testing and characterization. The structural analysis of the HEAs was conducted using X-ray diffraction (XRD) with a Cu-K $\alpha$  ( $\lambda = 1.5406 \text{ \AA}$ ) radiation source. The crystallite size and lattice strain were estimated using Eq. (1) and Eq. (2), respectively [16, 17].

$$D = \frac{K\lambda}{\beta \cos\theta} \quad (1)$$

$$\varepsilon = \frac{\beta}{4 \tan\theta} \quad (2)$$

where  $D$  is crystallite size,  $\varepsilon$  is degree of lattice strain,  $\beta$  is peak broadening,  $K$  is correction shape factor,  $\lambda$  is wavelength of the incident radiation, and  $\theta$  is diffraction angle. The influence of microstructures on hardness was utilized to examine the mechanical changes as a function of Sm addition, annealing temperature, and annealing time. A microhardness tester with a 50 g load and a dwell time of 10 s was used to determine the hardness. The standard deviations were calculated from at least 8 successful measurements.

## 3. RESULTS AND DISCUSSION

**Figure 1** displays the XRD scans of (a) CoCrFeNi, (b) (CoCrFeNi)<sub>99</sub>Sm<sub>1</sub>, and (c) (CoCrFeNi)<sub>98</sub>Sm<sub>2</sub> HEAs after MA and annealing at 700 °C, 900 °C, and 1100 °C for 1 h and 24 h. The figure shows that the MA of elemental powders resulted in a solid solution phase with a face-centered cubic (fcc) crystal structure. The thermo-physical calculations clarified that the entropy of mixing, atomic size difference, and enthalpy of mixing values support the formation of the single-phase fcc solid solution [18]. Moreover, the inclusion of 1% and 2% Sm did not seem to impact the as-milled crystal structure, likely due to the formation of a solid solution and the low concentration. That being said, the formation of chromium oxide and chromium carbide was observed after annealing, with their intensity varying based on annealing temperatures and times.

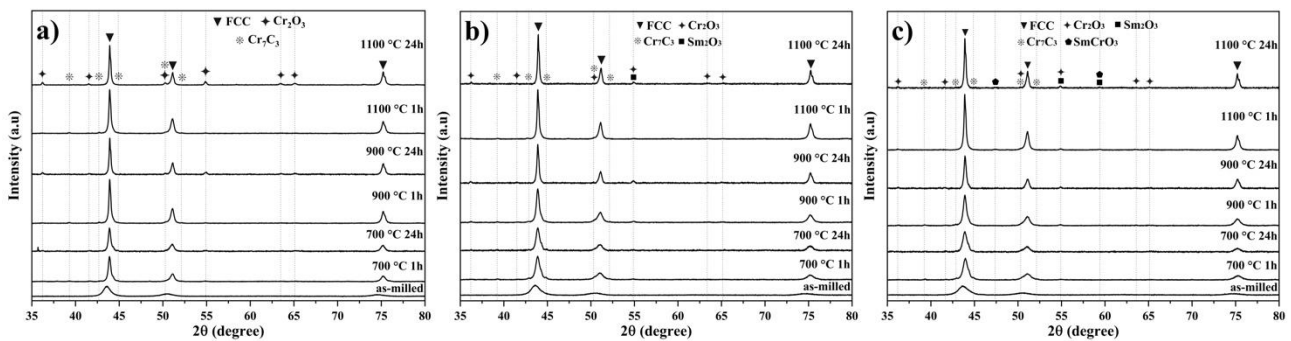


**Figure 1** The XRD scans of (a) CoCrFeNi, (b) (CoCrFeNi)<sub>99</sub>Sm<sub>1</sub>, and (c) (CoCrFeNi)<sub>98</sub>Sm<sub>2</sub> HEAs as a function of annealing temperature and annealing time

The addition of PCA to eliminate cold welding during MA and the contaminations during powder processing can promote the formation of such phases when exposed to elevated temperatures [19]. Additionally, Sm-

based oxide phases are observed to form upon annealing of  $(\text{CoCrFeNi})_{98}\text{Sm}_2$  and  $(\text{CoCrFeNi})_{99}\text{Sm}_1$  HEAs. It has been reported that  $\text{Sm}_2\text{O}_3$  phase forms due to the active chemical properties of samarium, which may also interact with  $\text{Cr}_2\text{O}_3$  at elevated temperatures to form  $\text{SmCrO}_3$  phase [20, 21]. The broad diffraction peaks observed in the as-milled samples resulted from the refined grain size and increased lattice strain induced by high-energy MA [22]. This was further confirmed by analyzing the XRD peaks to determine the crystallite size and lattice strains after MA and annealing. For example, the as-milled crystallite size was found to be less than 10 nm, which is consistent with the values reported for the mechanically alloyed CoCrFeNi HEA [23]. Additionally, MA promotes the formation of nano-sized grains, creates complex grain boundary structures, and introduces excess point defects and dislocations into the microstructure, all of which contribute to increased lattice strain [24]. The calculations shown in **Figure 2** reveal a high lattice strain of 1.17% in CoCrFeNi HEA. With the addition of Sm, having a larger atomic radius than the matrix atoms, the strain increased to 1.33% and 1.41% for  $(\text{CoCrFeNi})_{99}\text{Sm}_1$  and  $(\text{CoCrFeNi})_{98}\text{Sm}_2$ , respectively, resulting in higher lattice distortion [25].

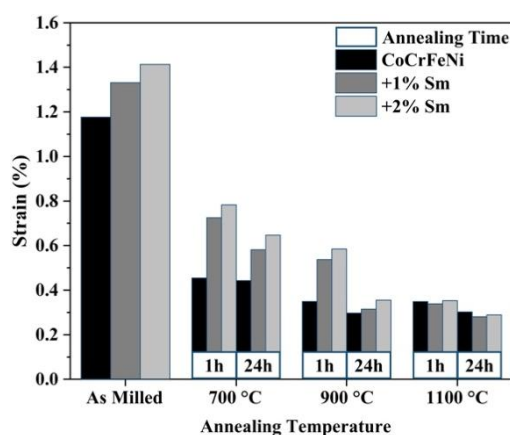


**Figure 2** The strain values of the investigated HEAs after MA and annealing

Nevertheless, the broad diffraction peaks observed in the as-milled HEAs, which resulted from the refined grain size and increased lattice strain due to the high-energy MA process, became sharper after annealing, as shown in **Figure 1**. This sharpening is attributed to strain relaxation and some degree of grain coarsening. It has been reported that during the annealing of nanocrystalline materials, the boundary structures evolve, excess vacancy complexes are removed, and dislocations are reorganized, which is expected to decrease the lattice strain [26]. Accordingly, annealing of the as-milled HEAs reduced the lattice strains as seen in the figure. That is, the lattice strain of CoCrFeNi HEA was reduced to 0.45% and 0.30% after 1h annealing at 700 °C and 24 h annealing at 1100 °C. Although a reduction in lattice strain was also observed for Sm-added HEAs with increased annealing temperatures and extended annealing times, the lattice strain of  $(\text{CoCrFeNi})_{99}\text{Sm}_1$  and  $(\text{CoCrFeNi})_{98}\text{Sm}_2$  HEAs remained higher up to 900 °C and 24 h annealing, as shown in **Figure 2**. However, at 1100 °C, the lattice strains of all investigated HEAs appear comparable, suggesting that the Sm atoms were completely rejected from the crystal structure of CoCrFeNi HEA.

The relationship between hardness and microstructural evolution was used to assess the mechanical properties. The grain size, estimated from XRD scans, is also presented in **Figure 3 (a)**. It should be noted that the estimation of grain size using the Scherrer equation may be inconsistent for larger grain sizes at high annealing temperatures. Therefore, it was applied to determine the grain size of as-milled HEAs and those annealed at low temperatures. The microhardness test results of CoCrFeNi,  $(\text{CoCrFeNi})_{99}\text{Sm}_1$ , and  $(\text{CoCrFeNi})_{98}\text{Sm}_2$  are given in **Figure 3 (b)** as a function of temperature after 1 h annealing, (c) as a function of time at 900 °C up to 24 h, and (d) as a function of time at 1100 °C up to 24 h. The as-milled CoCrFeNi hardness was measured as  $517.8 \pm 25$  HV, over three times higher than that of conventionally cast CoCrFeNi

[27], which can be attributed to grain size refinement and increased dislocation density induced by the (MA) [28].

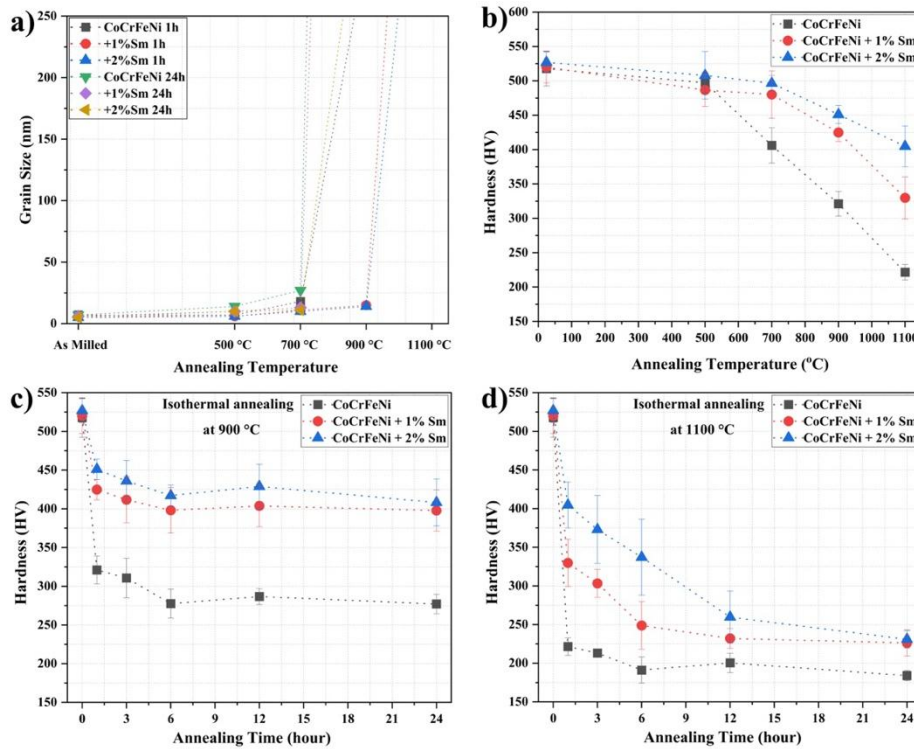


**Figure 3** (a) grain size and (b-d) hardness of the investigated HEAs as a function of Sm addition, annealing temperature, and annealing time

Additionally, the as-milled hardness of CoCrFeNi further increased to  $520 \pm 22$  HV and  $527 \pm 15$  HV with 1% and 2% Sm additions, respectively, likely due to the distortion of the fcc crystal lattice and dislocation pinning from local lattice strains within the grains [29]. As shown in **Figure 3(a)**, annealing is expected to promote grain growth, which in turn reduces hardness. The  $517.8 \pm 25$  HV as-milled hardness of CoCrFeNi showed a slight decrease to  $406 \pm 25$  HV at 700 °C but experienced a dramatic reduction to  $221.5 \pm 11$  HV at 1100 °C. The addition of Sm shifted the reduction in hardness to higher temperatures and made the reduction more gradual. For example, the hardness of  $(\text{CoCrFeNi})_{98}\text{Sm}_2$  HEA was  $496 \pm 11$  HV at 700 °C and  $404.5 \pm 30$  HV at 1100 °C, with the retention of higher hardness attributed to the nanocrystalline grain size [9] and the formation of Sm-based additional oxide phases [30]. Sm-added HEAs also show higher hardness and better stability upon extended annealing times up to 24 h at 900 °C, as seen in **Figure 3 (c)**. That is, the hardness of CoCrFeNi decreased from  $517.8 \pm 25$  HV to  $277 \pm 13$  HV, while the hardness of  $(\text{CoCrFeNi})_{98}\text{Sm}_2$  reduced from  $527 \pm 15$  HV to  $408.2 \pm 30$  HV after 24 h of annealing at 900 °C. However, all HEAs experienced dramatic hardness reductions after extended annealing times at 1100 °C, regardless of Sm content, as illustrated in **Figure 3 (d)**. Specifically, the hardness of CoCrFeNi,  $(\text{CoCrFeNi})_{99}\text{Sm}_1$ , and  $(\text{CoCrFeNi})_{98}\text{Sm}_2$  HEAs decreased to  $184 \pm 6$  HV,  $226 \pm 17$  HV, and  $231 \pm 11$  HV, respectively, after 24 h of annealing 1100 °C. This is attributed to grain growth in the microstructure and particle coarsening, which yields larger interparticle spacing and less hardening, according to Orowan strengthening.

#### 4. CONCLUSION

The effect Sm on the structural and hardness stability of nanocrystalline CoCrFeNi HEAs was thoroughly investigated. The results indicated that the as-milled hardness of CoCrFeNi, initially measured as  $517.8 \pm 25$

HV, decreased significantly to  $221.5 \pm 11$  HV and  $184 \pm 6$  HV, after 1 h and 24 h annealing at 1100 °C, respectively, resulting in reductions of 57% and 65%, respectively. This suggests that the nanocrystalline CoCrFeNi HEA is not mechanically stable at elevated temperatures. However, while a significant reduction in hardness was observed at 1100 °C when annealed up to 24 h, the experimental results indicate that the Sm addition helps CoCrFeNi HEA retain its high hardness even after 24 h of annealing at 900 °C. This is attributed to the presence of the rare earth element Sm and the formation of Sm-based mixed oxide phases. These findings highlight the potential to improve the mechanical stability of nanocrystalline CoCrFeNi HEAs during high-temperature processing, such as sintering the as-milled HEA powders.

## ACKNOWLEDGEMENTS

***This study was supported by the Scientific and Technological Research Council of Turkey (TUBITAK) under Grant Number 222M218. The authors thank TUBITAK for their support.***

## REFERENCES

- [1] YEH, J.W., CHEN, S.K., LIN, S.J., GAN, J.Y., CHIN, T.S., SHUN, T.T., TSAU, C.H., CHANG, S.Y. Nanostructured high-entropy alloys with multiple principal elements: Novel alloy design concepts and outcomes. *Adv. Eng. Mater.* 2004, Vol. 6, No. 5, pp. 299-303.
- [2] KUMAR, A., ARORA, A., CHANDRAKAR, R., RAO, K.R., CHOPKAR, M. Nano-crystalline high entropy alloys prepared by mechanical alloying. *Mater. Today Proc.* 2020, Vol. 27, pp. 1310-1314.
- [3] KOCH, C.C., SCATTERGOOD, R.O., YOUSSEF, K.M., CHAN, E., ZHU, Y.T. Nanostructured materials by mechanical alloying: new results on property enhancement. *J. Mater. Sci.* 2010, Vol. 45, pp. 4725-4732.
- [4] KIRCHHEIM, R. Reducing grain boundary, dislocation line and vacancy formation energies by solute segregation. I. Theoretical background. *Acta Mater.*, 2007, Vol. 55, No. 15, pp. 5129-5138.
- [5] KOTAN, H., TEKIN, M., BAYATLI, A., BAYRAK, K.G., KOCABAŞ, M., AYAS, E. Effect of in-situ formed oxide and carbide phases on microstructure and corrosion behavior of Zr/Y doped CoCrFeNi high entropy alloys prepared by mechanical alloying and spark plasma sintering. *Intermetallics*. 2023, p. 162.
- [6] ZAMANI, M.R., MIRZADEH, H., MALEKAN, M., CAO, S.C., YEH, J.-W. Grain growth in high-entropy alloys (HEAs): A review. *High Entropy Alloys & Materials*. 2023, Vol. 1, No. 1, pp. 25-59.
- [7] PRAVEEN, S., MURTY, B., KOTTADA, R.S. Phase evolution and densification behavior of nanocrystalline multicomponent high entropy alloys during spark plasma sintering. *JOM*. 2013, Vol. 65, No. 12, pp. 1797-1804.
- [8] JIANG, H., HAN, K., QIAO, D., LU, Y., CAO, Z., LI, T. Effects of Ta addition on the microstructures and mechanical properties of CoCrFeNi high entropy alloy. *Mater. Chem. Phys.* 2018, Vol. 210, pp. 43-48.
- [9] KOTAN, H., KOÇ, R.C., BATIBAY, A.B. Remarkable thermal stability of nanocrystalline CoCrFeNi high entropy alloy achieved through the incorporation of rare-earth element samarium. *Intermetallics*. 2025, p. 108608.
- [10] KOCH, C., SCATTERGOOD, R., DARLING, K., SEMONES, J. Stabilization of nanocrystalline grain sizes by solute additions. *J. Mater. Sci.*, 2008, Vol. 43, pp. 7264-7272.
- [11] SCHUH, V., MENDEZ-MARTIN, F., VÖLKER, B., GEORGE, E.P., CLEMENS, H., PIPPAN, R., HOHENWARTER, A. Mechanical properties, microstructure and thermal stability of a nanocrystalline CoCrFeMnNi high-entropy alloy after severe plastic deformation. *Acta Mater.* 2015, Vol. 96, pp. 258-268.
- [12] POLAT, G., TEKİN, M., KOTAN, H. Role of yttrium addition and annealing temperature on thermal stability and hardness of nanocrystalline CoCrFeNi high entropy alloy. *Intermetallics*. 2022, p. 146.
- [13] ZHANG, L.J., YU, P.F., ZHANG, M.D., LIU, D.J., ZHOU, Z., MA, M.Z., LIAW, P.K., LI, G., LIU, R.P. Microstructure and mechanical behaviors of GdxCoCrCuFeNi high-entropy alloys. *Mater. Sci. Eng.* 2017, Vol. A 707, pp. 708-716.
- [14] MOAZZEN, P., TOROGHINEJAD, M.R., KARIMZADEH, F., VLEUGELS, J., RAVASH, H., CAVALIERE, P. Influence of zirconium addition on the microstructure, thermodynamic stability, thermal stability and mechanical properties of mechanical alloyed spark plasma sintered FeCoCrNi high entropy alloy. *Powder Metall.* 2018, Vol. 61, No. 5, pp. 405-416.

- [15] PENG, S., LU, Z., GAO, S., LI, H. Improved microstructure and mechanical properties of ODS-CoCrFeNiMn high entropy alloys by different Ti, Zr and Y<sub>2</sub>O<sub>3</sub> addition. 2023, Vol. 935, pp. 168166.
- [16] BABU, P.D., DONGRE, P., MOGANRAJ, A., MANIVASAGAM, G., SCHWANDT, C., SURE, J. Wear behavior of CoCrFeNi high-entropy alloy prepared by mechanical alloying. *J. Alloys Compd.* 2025, Vol. 1010, p. 177115.
- [17] SUN, M., YANG, Z., SONG, S., ZHANG, J., LU, B. Effect of Cr content on microstructure, mechanical, and corrosion properties of CoCr<sub>x</sub>FeMnNi high-entropy alloys fabricated by selective laser melting. *Mater Charact.* 2024, Vol. 212, p. 113949.
- [18] ANDREOLI, A.F., SHULESHOVA, O., WITUSIEWICZ, V.T., WU, Y., YANG, Y., IVASHKO, O., DIPPEL, A.-C., ZIMMERMANN, M.V., Nielsch, K., Kaban, I. In situ study of non-equilibrium solidification of CoCrFeNi high-entropy alloy and CrFeNi and CoCrNi ternary suballoys. *Acta Mater.* 2021, Vol. 212, p. 116880.
- [19] VAIDYA, M., ANUPAM, A., BHARADWAJ, J.V., SRIVASTAVA, C., MURTY, B. Grain growth kinetics in CoCrFeNi and CoCrFeMnNi high entropy alloys processed by spark plasma sintering. *J. Alloys Compd.* 2019, Vol. 791, pp. 1114-1121.
- [20] PRADO-GONJAL, J., SCHMIDT, R., ROMERO, J.-J., ÁVILA, D., AMADOR, U., MORÁN, E. Microwave-Assisted Synthesis, Microstructure, and Physical Properties of Rare-Earth Chromites. *Inorg. Chem.* 2013, Vol. 52, No. 1, pp. 313-320.
- [21] MENG, L., FANG, S., TAN, M., FU, W., KE, L. Microstructure and properties of typical equiatomic CrMnFeCoNi high entropy alloy doped with different rare earth elements. *Intermetallics.* 2024, Vol. 175, p. 08477.
- [22] CULLITY, B.D. Elements of X-ray Diffraction, Addison-Wesley Publishing 1956.
- [23] PRAVEEN, S., MURTY, B., KOTTADA, R.S. Phase evolution and densification behavior of nanocrystalline multicomponent high entropy alloys during spark plasma sintering. *JOM.* 2013, Vol. 65, pp. 1797-1804.
- [24] GLEITER, H. Nanostructured Materials. *Adv. Mater.* 1992, Vol. 4, No. 7-8, pp. 474-481.
- [25] LI, J., YAMANAKA, K., CHIBA, A. Significant lattice-distortion effect on compressive deformation in Mo-added CoCrFeNi-based high-entropy alloys. *Mater. Sci. Eng.* 2022, Vol. A 830, p. 142295.
- [26] RUPERT, T.J., TRELEWICZ, J.R., SCHUH, C.A. Grain boundary relaxation strengthening of nanocrystalline Ni-W alloys. *J. Mater. Res.* 2012, Vol. 27, No. 9, pp. 1285-1294.
- [27] WANG, J., GUO, T., LI, J.S., JIA, W.J., KOU, H.C. Microstructure and mechanical properties of non-equilibrium solidified CoCrFeNi high entropy alloy. *Mater. Chem. Phys.* 2018, Vol. 210, pp. 192-196.
- [28] ZHU, W.Q., GAO, X., YAO, Y.Y., HU, S.J., LI, Z.X., TENG, Y., WANG, H., GONG, H., CHEN, Z.Q., YANG, Y. Nanostructured High Entropy Alloys as Structural and Functional Materials. *ACS Nano.* 2024, Vol. 18, No. 20, pp. 12672-12706.
- [29] RUPERT, T.J., TRENKLE, J.C., SCHUH, C.A. Enhanced solid solution effects on the strength of nanocrystalline alloys. *Acta Mater.* 2011, Vol. 59, No. 4, pp. 1619-1631.
- [30] CHANG, H., ZHANG, T.W., MA, S.G., ZHAO, D., BAI, T.X., WANG, K., LI, Z.Q., WANG, Z.H. Strengthening and strain hardening mechanisms in precipitation-hardened CrCoNi medium entropy alloys. *J. Alloys Compd.* 2022, p. 896.